

# QED PROCESSES IN TWO PHOTON REACTIONS \*)

M. Pohl  
III. Phys. Inst. A  
R W T H Aachen, Germany

## ABSTRACT

I review experimental results on the reactions  $e^+e^- \rightarrow e^+e^-e^+e^-$  and  $e^+e^- \rightarrow e^+e^-\mu^+\mu^-$  from PETRA and PEP. Recent high statistics measurements are compared to QED predictions in the form of diagrammatic leading order ( $\alpha^4$ ) calculations and to the equivalent photon approximation. The leading order calculation describes the data well over the full kinematic range covered by experiments ( $0.1 \lesssim Q^2 \lesssim 100$   $GeV^2/c^2$ ). The "two photon interaction" graph is found to saturate the observed cross section. Only for small masses of the produced leptonic system, first indications of a bremsstrahlung type background are observed at the percent level. The leptonic structure function  $F_2^\gamma(x, Q^2)$  is measured and also agrees with the behavior expected from QED.

\*) Invited talk given at the 5th International Workshop on Photon Photon Collisions, Aachen, April 1983.

## 1. INTRODUCTION

Lepton pair production by the two photon process

$$e^+ e^- \rightarrow e^+ e^- e^+ e^- \quad (1)$$

$$e^+ e^- \rightarrow e^+ e^- \mu^+ \mu^- \quad (2)$$

is one of the few examples of a higher order ( $\alpha^4$ ) QED reaction that can be studied at large momentum transfers ( $Q^2$ ). A measurement of these processes at high energies therefore provides a test of QED complementary to the more conventional studies of higher orders at low  $Q^2$  (1) or first order at maximum  $Q^2$  (2).

Because of their logarithmic growth with the cms energy of the initial state ( $\sqrt{s}$ ), the total cross sections are large even at high energies. In present collider experiments, reaction (2) even dominates the first order process  $e^+ e^- \rightarrow \mu^+ \mu^-$  by several orders of magnitude. Most of this cross section, however, goes unobserved, since the bremsstrahlung nature of the process strongly aligns the reaction products with the incoming beams. Cross section measurements of two photon reactions therefore generally involve large extrapolation of the accessible kinematic range. A detailed analysis of data on these calculable "gauge reactions" allows one to study the reliability of such extrapolations.

It is mainly because of these two reasons that almost all experiments at PETRA and PEP are presenting high statistics measurements of

reactions (1) and/or (2). The kinematic variables used in characterizing the data are displayed in Fig. 1. When the momentum  $Q_i^2$  transferred to both electrons is small, only the produced lepton pair can be observed. In this "no tag" case, the mass  $W$  of the system and the transverse momentum  $p_{\perp}$  of the particles are

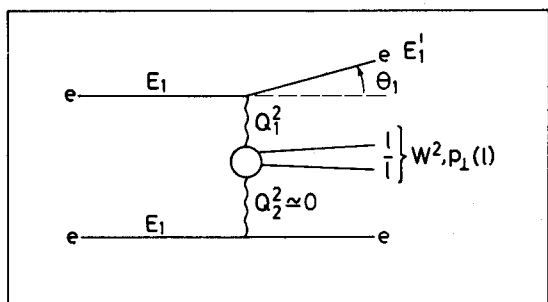


Fig. 1

measured. In the comparatively rare case where one of the photons is sufficiently off shell such that the radiating electron is "tagged" in the detector, also its momentum transfer can be measured and the kinematics are completely determined to the extent that the second photon is real.

The experimental conditions and statistics for the data included in this report are summarized in Table I. The  $Q^2$  range covered by the experiments is shown in Fig. 2. It can be seen that detectors are rather complementary and that the accessible momentum transfers range all the way from  $Q^2 \approx 0.1 \text{ GeV}^2/c^2$  to  $100 \text{ GeV}^2/c^2$ .

Experiment	$\int L dt$ $\text{pb}^{-1}$	$\langle \sqrt{s} \rangle$ GeV	Final State	Number of Events no tag	Number of Events tag	Tag Device
CELLO	7.5	34	eeee		130	EC
			ee $\mu\mu$		111	EC
MARK-J	85.8	34	ee $\mu\mu$	2861	(132)	CD
PLUTO	40	35	ee $\mu\mu$	987	537	SA
					345	LA
					100	EC
TASSO	19.3	33	ee $\mu\mu$		127	EC
MAC	25	29	ee $\mu\mu$	2763		-
PEP-9/ TPC	3	29	ee $\mu\mu$		421	SA

Table I

Statistics and experimental conditions for the data included in this report. Tagging devices used are small angle taggers (SA), large angle taggers (LA), calorimeter end caps (EC), and central detectors (CD).

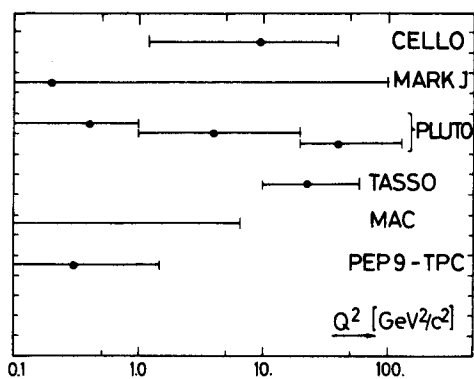


Fig. 2

The QED calculations used to compare to the data are twofold. Exact diagrammatic calculations to lowest order<sup>(3)</sup> exist in form of a Monte Carlo integration program and event generator and allow for detailed studies taking into account the detector response.

The types of diagrams considered are schematically shown in Fig. 3. According to QED, the lepton pair production is dominated by the "two photon" graph with charge parity  $C = +1$ . A contribution at the percent level comes from the t-channel bremsstrahlung diagram with  $C = -1$ . Bremsstrahlung from the s-channel is negligible. Bremsstrahlung contributions may be found experimentally by looking at low mass lepton pairs or by searching for a small charge asymmetry in the produced leptons due to interference between the two graphs with opposite  $C$  parity. Calculations of higher order corrections ( $\alpha^5$ ) are in progress<sup>(4)</sup>. First indications are that they are very small and can safely be neglected at the present level of experimental accuracy.

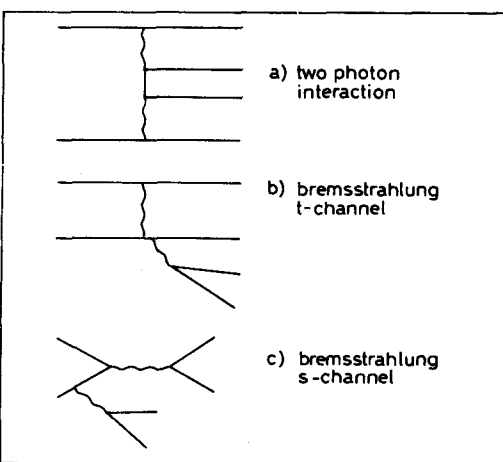


Fig. 3

Given the dominance of the two photon interaction diagram, the cross section can also be calculated in the equivalent photon approximation (EPA)<sup>(5)</sup>. In that case the photon flux<sup>(6)</sup> coming from an incident electron is convoluted with the cross section for  $e\gamma$  scattering. If both photons are quasi-real, the photon flux from both electrons may be convoluted with the cross section for  $\gamma\gamma$  scattering (double equivalent photon approximation, DEPA)<sup>(7)</sup>.

## 2. GENERAL PROPERTIES OF $e^+e^- \rightarrow e^+e^-\ell^+\ell^-$

Since two photon interactions are a bremsstrahlung phenomenon, both initial state photons are of low energy and strongly aligned with the incoming  $e^\pm$  beams. Moreover, the lepton pair production cross section in the  $\gamma\gamma$  center of mass system

$$\frac{d\sigma(\gamma\gamma \rightarrow \ell\bar{\ell})}{d\cos\theta^*} \sim \frac{1 + \cos^2\theta^*}{1 - \cos^2\theta^*} \quad (3)$$

is strongly peaked along the photon direction. The observable fraction of cross section in a storage ring experiment is therefore at the percent level. Fig. 4 shows the observed cross section as a function of  $\sqrt{s}$  for  $e^+e^- \rightarrow e^+e^-\mu^+\mu^-$  in the MARK-J experiment. It becomes

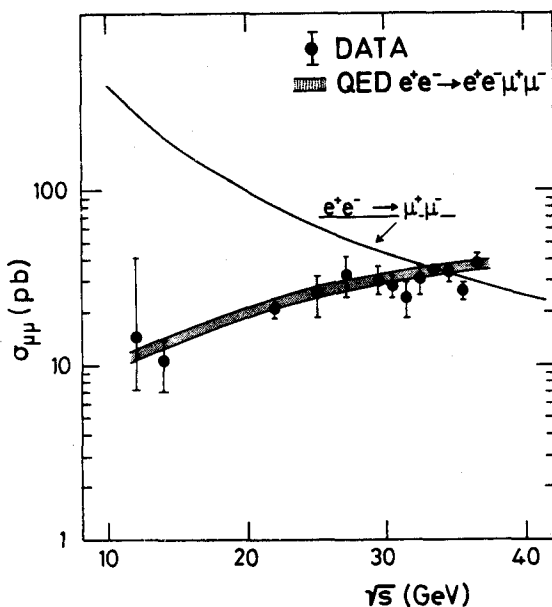


Fig. 4

Fig. 6 compares the acolinearity and acoplanarity distributions observed in two-photon muon pairs to the QED prediction including detector resolution. While the boost of the  $\gamma\gamma$  cms tends to make the muons acolinear, they stay largely coplanar since under "no tag" conditions the transverse momentum carried away by the electrons is limited.

comparable to the one photon exchange cross section (of which  $\sim 60\%$  are observable) only at the highest PETRA energies. The two processes can, however, easily be separated even if no tagged electron is observed. Fig. 5 shows the momentum spectrum of muon pairs measured in MARK-J. The peak at  $P_\mu/P_{\text{beam}} \approx 1$ , due to the one-photon process, is clearly separated from the low energy muons produced by two photon interactions.

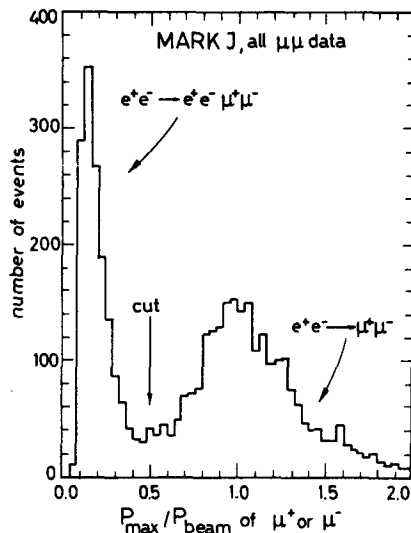


Fig. 5

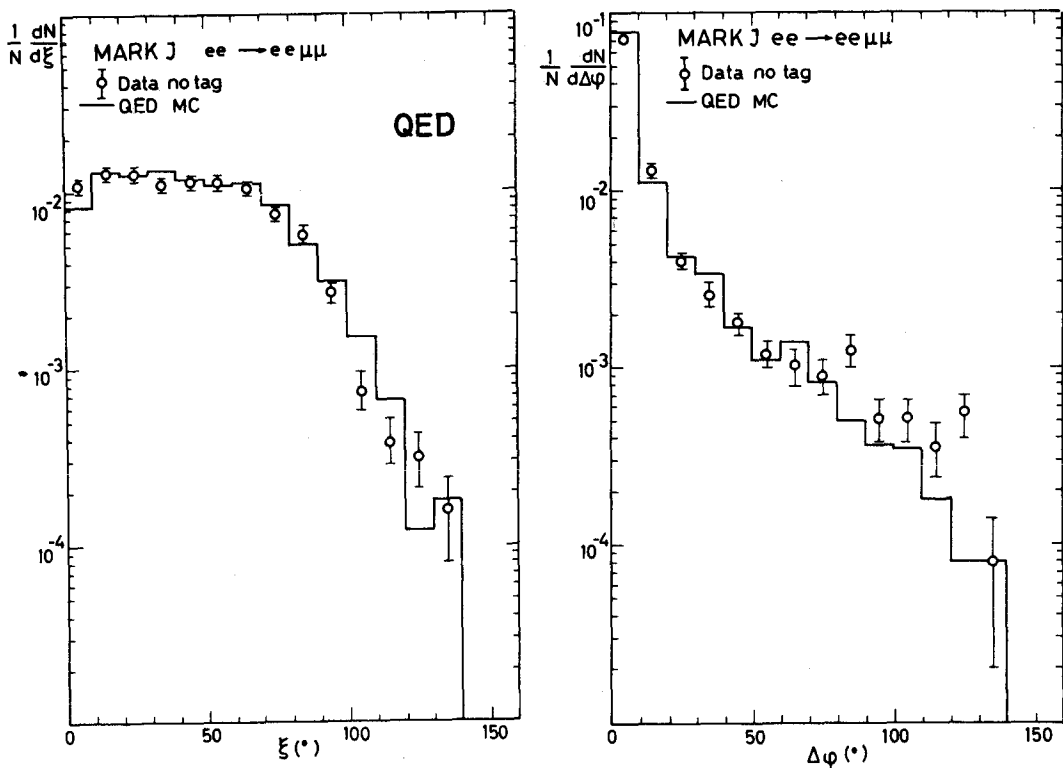


Fig. 6

### 3) UNTAGGED LEPTON PAIR PRODUCTION

In the case where none of the initial electrons is scattered into the detector, it is difficult to disentangle the two photon process  $e^+e^- \rightarrow e^+e^-e^+e^-$  from radiative Bhabha scattering  $e^+e^- \rightarrow e^+e^-\gamma$ . Data under "no tag" conditions are therefore only available for muon pair production.

Fig. 7 shows the uncorrected mass distribution of two photon muon pairs observed by MARK-J and PLUTO at PETRA ( $\sqrt{s} \approx 34$  GeV) and by MAC at PEP ( $\sqrt{s} = 29$  GeV). The data are compared to a QED ( $\alpha^4$ ) Monte Carlo calculation<sup>(3)</sup> which takes into account the detector acceptance and resolution. The agreement is very satisfactory up to the highest masses accessible. No indication for a new state with  $C = +1$  decaying into  $\mu^+\mu^-$  is seen in the mass range covered.

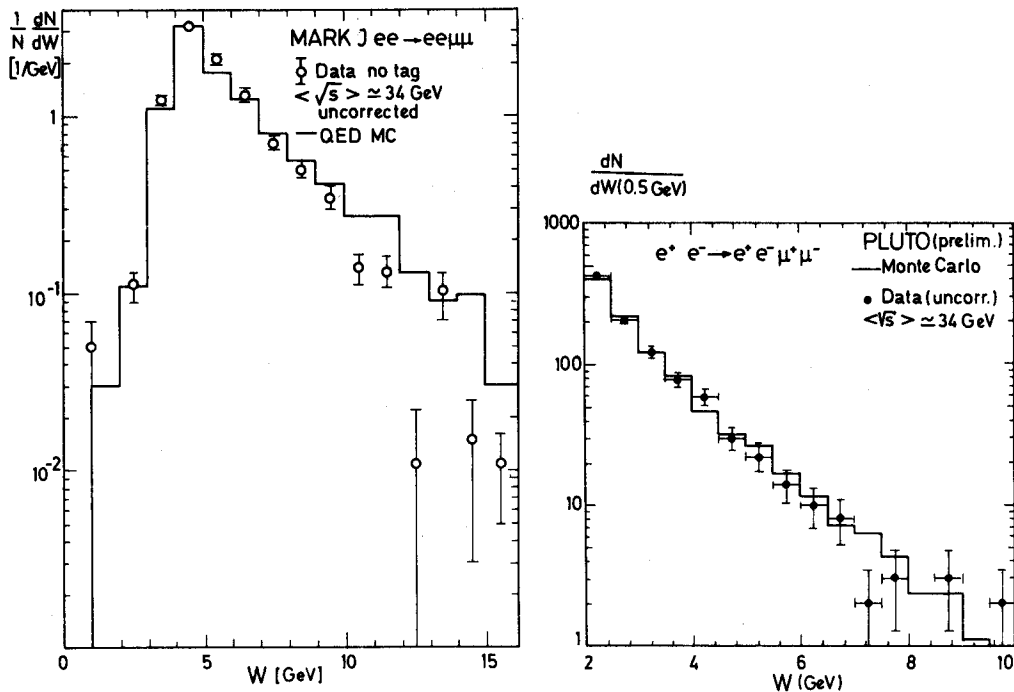
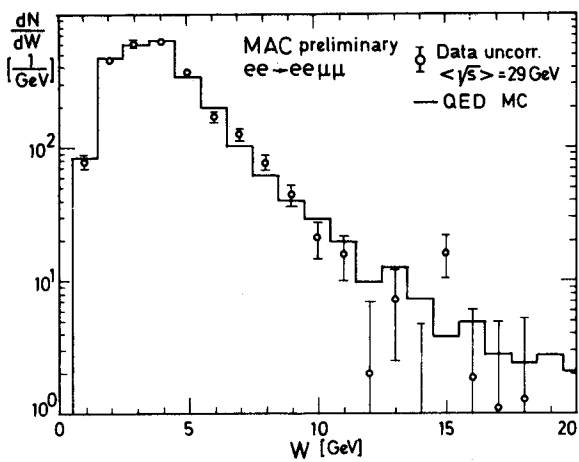


Fig. 7



The agreement between data and leading order QED Monte Carlo after detector response simulation allows one to apply a bin-wise acceptance correction to the data. This has been done for the data in Fig. 8 which displays the differential cross section as a function of the muon

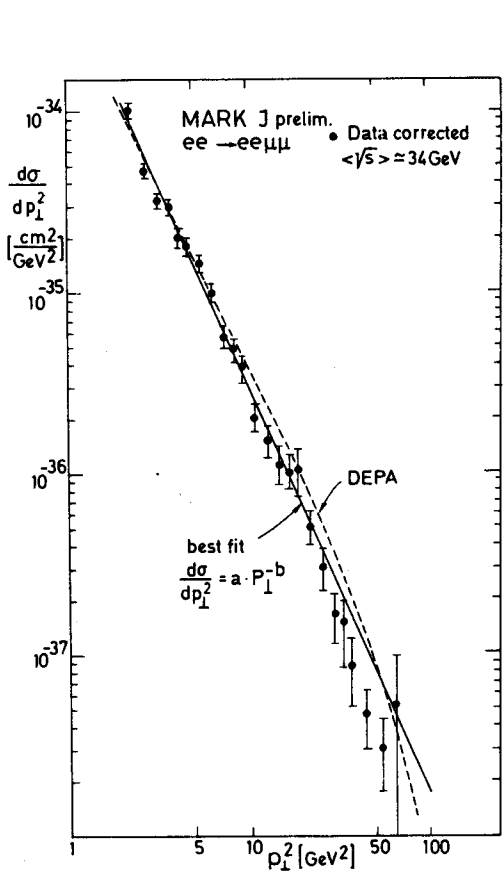


Fig. 8

the best fit parameters are

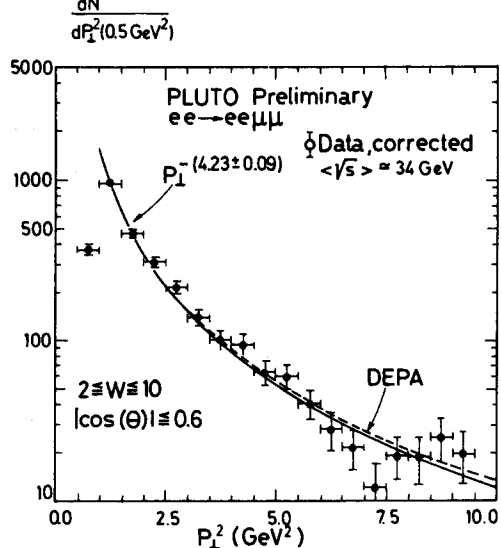
$$a = 5.43 \pm 0.90 \text{ (stat)} \pm 0.50 \text{ (syst)} \quad \text{nb}/(\text{GeV}^2/\text{c}^2) \quad (5)$$

$$b = 4.47 \pm 0.21 \text{ (stat)} \pm 0.25 \text{ (syst)}$$

QED predicts an exponent  $b = 4.54$  in good agreement with the observation. The preliminary PLUTO data have an average  $Q^2$  of  $0.01 \text{ GeV}^2/\text{c}^2$  and cover  $|\cos\theta_\mu| < 0.60$ . The exponent is fitted to be

$$b = 4.23 \pm 0.09 \text{ (stat)} \quad (6)$$

also in good agreement with the QED prediction of 4.19 calculated for their conditions.



transverse momentum  $P_\perp$  with respect to the beam line. The data fit well to a power law

$$\frac{d\sigma}{dp_\perp^2} = a \cdot p_\perp^{-b} \quad (4)$$

In the case of the MARK-J data, taken at an average  $Q^2$  of  $0.2 \text{ GeV}^2/\text{c}^2$  and for  $|\cos\theta_\mu| < 0.86$ ,

Also shown in Fig. 8 are the predictions of a DEPA calculation<sup>(7)</sup> which describes the data equally well. The double equivalent photon approximation is thus applicable under "no tag" conditions as it is expected to be.

#### 4) TAGGED LEPTON PAIR PRODUCTION

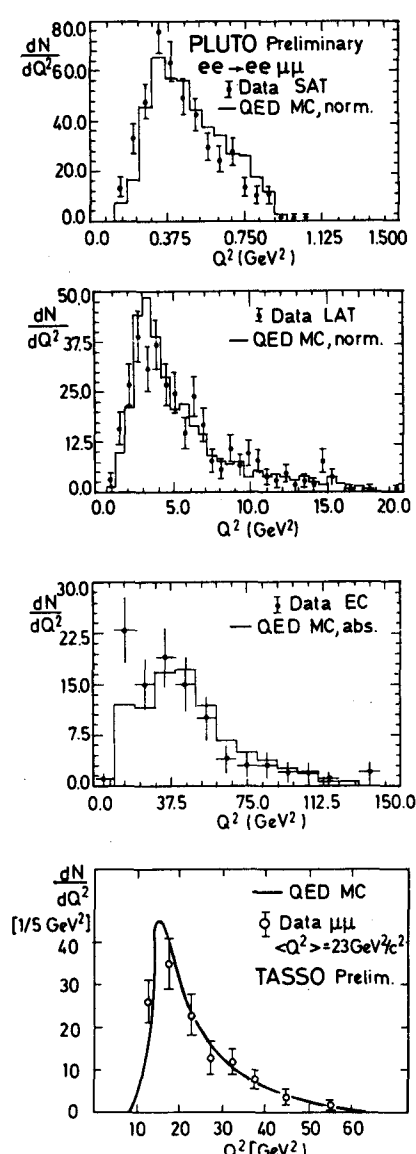
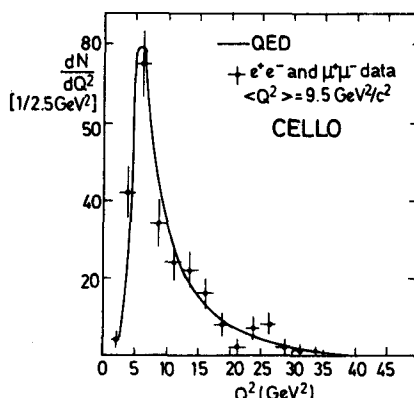


Fig. 9

In the case of a tagged electron, the mass  $Q^2$  of the projectile photon is measured, while the target photon remains almost real. Fig. 9 shows the  $Q^2$  distributions observed in the CELLO, PLUTO and TASSO experiments at PETRA. In the CELLO data<sup>(8)</sup>, the processes  $e^+e^- \rightarrow e^+e^-$  and  $e^+e^- \rightarrow e^+e^- \mu^+\mu^-$  are plotted together since their kinematic properties are very similar. All other groups restrict themselves to muon pair production. Fig. 9 substantiates the  $Q^2$  range of the experiments already indicated in Fig. 2. The agreement of the data to the leading order QED Monte Carlo predictions is very good.

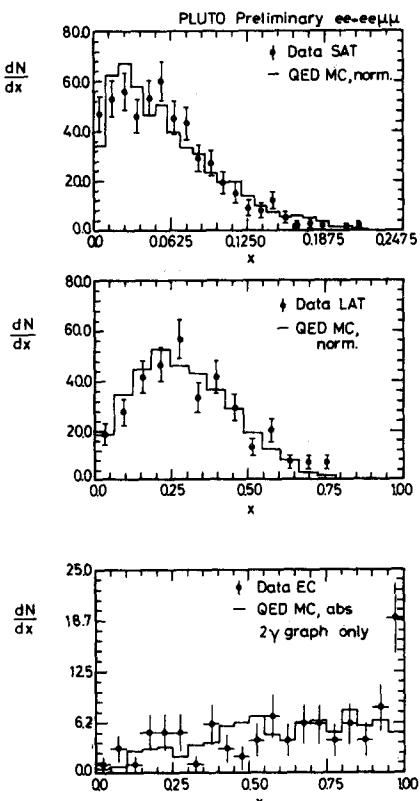
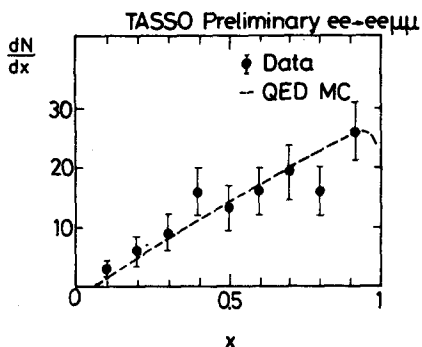
Since the momentum transfer  $Q^2$  and the mass of the lepton system  $W^2$  are simultaneously measured, the "scaling" variable

$$x = \frac{Q^2}{Q^2 + W^2} \quad (7)$$



can be inferred. Experimental results are shown in Fig. 10. The agreement with QED is again generally good. An interesting aspect is seen in the PLUTO data where the high  $Q^2$  data are compared to an absolute QED prediction considering only the "two-photon" graph of Fig. 3a. An excess of events at  $x \approx 1$  ( $W^2 \approx 0$ ) is observed. It can be attributed to events from virtual bremsstrahlung, Fig. 3b, which are of course expected to have a small muon pair mass. The candidates observed represent roughly 1% of the observed cross section which is also the correct order of magnitude for bremsstrahlung contributions.

Fig. 10



## 5) "LEPTONIC STRUCTURE" OF THE PHOTON

As mentioned briefly in the introduction, the lepton pair production by two photons is an important gauge reaction used to study and gain confidence in methods subsequently applied to other two photon reactions, like  $e^+e^- \rightarrow e^+e^- q\bar{q}$ , which are less well understood theoretically as well as experimentally. This especially applies to the structure function formalism. Unlike the hadronic structure function of the photon, its leptonic structure function can be reliably calculated in QED. Moreover, all relevant final state particles are observed and their momenta measured such that no experimental problems like

unfolding the "true" kinematics from the visible ones occur.

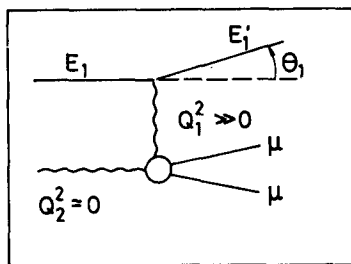


Fig. 11

For the sake of this test we pretend that we know nothing about the point-like coupling of the two photons to the lepton pair. We treat the process as deep inelastic scattering of an electron off a quasi-real photon, as shown in Fig. 11. We parametrize<sup>(5)</sup> the cross section in terms of structure functions  $F_1(x, Q^2)$  and  $F_2(x, Q^2)$ . It then takes the general form

$$\frac{d^2\sigma}{dx dQ^2} = \frac{4\pi\alpha^2}{Q^4 x} \{ (1-y)F_2^Y + xy^2 F_1^Y \} \quad (8)$$

where

$$y = 1 - E_1'/E_1 \cos^2 \frac{\theta_1}{2} \quad (9)$$

is the relative energy transfer.

It is clear from equation (8) that experiments will have no sensitivity to  $F_1$ , unless low tagging energy thresholds  $E_{\min}^1$  and minimum angles  $\theta_{\min}$  are accepted. This is demonstrated in Fig. 12 with a Monte Carlo study of the  $y$  distributions resulting from the  $F_2$  and  $xF_1$  term

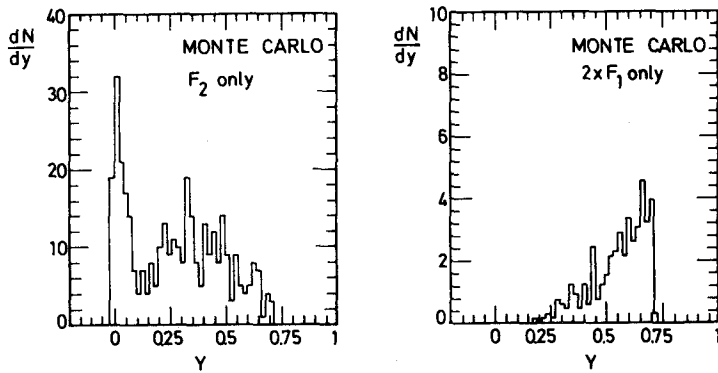


Fig. 12

in equation (8). An experimental  $y$  distribution from PEP-9 is shown in Fig. 13. It is evident that under present conditions, only  $F_2$  can be efficiently extracted from the data. Fig. 14 shows the results from CELLO and PEP-9 at  $\langle Q^2 \rangle$  of  $9.5 \text{ GeV}^2/\text{c}^2$  and  $0.3 \text{ GeV}^2/\text{c}^2$ , respectively.

Since the measured  $F_2^Y$  is averaged over the  $Q^2$  range accepted, the observed difference is explained by the  $Q^2$  dependence of the structure function.

Neglecting the mass of the target photon, QED predicts<sup>(5)</sup>

$$F_2^Y(x, Q_1^2) = \frac{\alpha}{\pi} x \{ [x^2 + (1-x)^2] \}$$

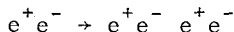
$$\ln \frac{Q_1^2 (\frac{1}{x} - 1)}{m_\mu^2} - 1 + 8x(1-x) \}$$

(10)

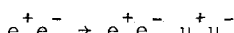
The corresponding curves are also shown in Fig. 14. The differences between the two measurements are thus quantitatively understood by the  $\ln Q^2$  dependence of the structure function. The agreement with QED is good.

### CONCLUSIONS

The recently accumulated high statistics data on



and



from experiments at PETRA and PEP agree with the expectations from leading order ( $\alpha^4$ ) calculations in QED. The data cover a  $Q^2$  range  $0.1 \lesssim Q^2 \lesssim 100 \text{ GeV}^2/c^2$ , and are taken under "no tag" as well as "single tag" conditions. The no tag cross sections are also well described by an analytical calculation based on the double equivalent

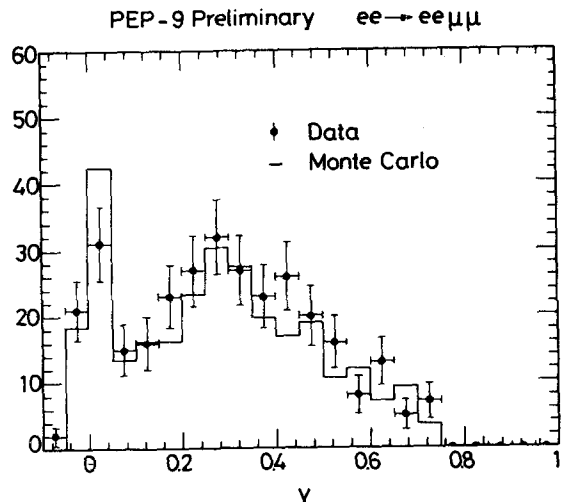


Fig. 13

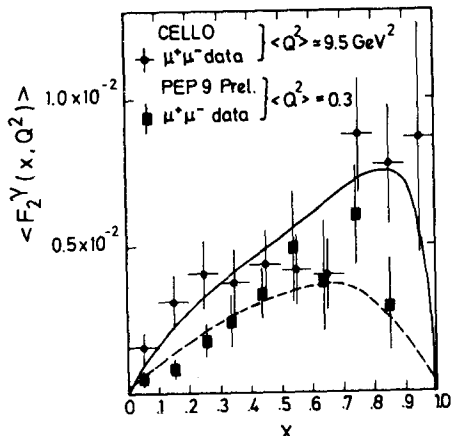


Fig. 14

photon approximation. Under most conditions, the "two-photon interaction" graph alone adequately accounts for the data. Only at  $x \approx 1$ , a "bremsstrahlung" background at the percent level is observed. The structure function approach gives an appropriate description of the data on  $e\gamma \rightarrow e\mu\mu$ . The measured "muonic" structure function  $\langle F_2^Y(x, Q^2) \rangle$  agrees with the behavior expected from QED.

#### ACKNOWLEDGEMENTS

I would like to thank the organizers of this conference, especially Prof. Ch. Berger, for creating such an informal atmosphere at this meeting. I am indebted to my colleagues from the PETRA and PEP experiments, especially Profs. E. Hilger, F.J. Kirschfink, W. Ko, K. Lau, G. Swider, A. Tylka and C. Williams for providing me with preliminary data prior to publication. I also thank the directors of DESY, Prof. V. Soergel and Prof. P. Söding for their hospitality.

#### REFERENCES

- (1) J. Builey et al., Nucl. Phys. B150, 1 (1979).  
R.S. Van Dyck, P.B. Schwingberg and H.G. Dehmelt, Phys. Rev. Lett. 38, 310 (1979).  
K. von Klitzing, G. Dorda and M. Pepper, Phys. Rev. Lett. 45, 494 (1980).
- (2) H.J. Behrend et al., Z. Phys. C16, 301 (1983).  
W. Bartel et al., Phys. Lett. 108B, 160 (1982) and DESY 83-035.  
B. Adeva et al., Phys. Rev. Lett. 48, 1701 (1982).  
Ch. Berger et al., Phys. Lett. 99B, 292 (1981).  
R. Brandelik et al., Phys. Lett. 117B, 365 (1982).  
E. Fernandez et al., Phys. Rev. Lett. 50, 1238 (1983).
- (3) R. Bhattacharya, J. Smith and G. Grammer, Phys. Rev. D15, 3267 (1977).  
J.A.M. Vermaseren, Proc. of the Int. Workshop on  $\gamma\gamma$  Collisions, Amiens 1980, G. Cochard and P. Kessler Eds., Lecture Notes in Physics 134, 35 (1980).  
S. Kawabata, see J. Field, Proc. of the 4th Int. Workshop on Photon-Photon Interactions, G.W. London Edt., Paris 1981, p. 447.
- (4) J.A.M. Vermaseren, Contribution to this conference.  
Ph. Daverveldt, Contribution to this conference.
- (5) see V.M. Buchner, I.F. Ginzburg, G.V. Meledin and V.G. Serbo, Phys. Rep. 15, 181 (1975).
- (6) J.H. Field, Nucl. Phys. B168, 477 (1980); B176, 345 (1980).  
Ch. Berger and J.H. Field, Nucl. Phys. B187, 585 (1981).
- (7) A. Coureau, CAL 82/19 (1982).
- (8) CELLO Collaboration, H.J. Behrend et al., DESY 83/017 (1983).

FIGURE CAPTIONS

Fig. 1 Kinematic variables used to study lepton pair production by two photon interactions.

Fig. 2  $Q^2$  range covered by the data included in this report.

Fig. 3 Types of Feynman graphs taken into account in the diagrammatic calculations of Ref. 3.

Fig. 4 Observed cross section for  $e^+e^- \rightarrow e^+e^-\mu^+\mu^-$  (no tag) from MARK-J as a function of center of mass energy.

Fig. 5 Maximum muon momentum measured by MARK-J in all events with two muons. The one photon and two photon production processes are clearly separated.

Fig. 6 Acolinearity ( $\xi$ ) and acoplanarity ( $\Delta\phi$ ) distributions for two photon muon pairs from MARK-J.

Fig. 7 Observed mass distribution for two photon muon pairs from MARK-J, PLUTO, and MAC, compared to the QED prediction including detector acceptance and resolution.

Fig. 8 Corrected cross section  $d\sigma/dp_T^2$  for two photon muon pairs (no tag) from MARK-J and PLUTO. The data are compared to a DEPA calculation and fitted to a power law.

Fig. 9  $Q^2$  distribution of single tag data from CELLO, PLUTO (small angle, large angle and end cap calorimeter tags) and TASSO. Data from CELLO include electron pair production.

Fig. 10  $x$  distribution of single tag data from PLUTO and TASSO.

Fig. 11 Kinematic variables used to study  $e\gamma$  scattering.

Fig. 12 A Monte Carlo study from the PEP 9 group showing the contributions of the  $F_2$  term and the  $x F_1$  term to be observed  $y$  distribution. Note the difference in vertical scale for the two graphs.

Fig. 13 Observed  $\gamma$  distribution from PEP 9 compared to the QED prediction.

Fig. 14 The muonic structure function  $F_2^{\gamma}(x, Q^2)$  as measured by CELLO ( $\langle Q^2 \rangle \approx 9.5 \text{ GeV}^2/c^2$ ) and PEP 9 ( $\langle Q^2 \rangle \approx 03. \text{ GeV}^2/c^2$ ), averaged over the  $Q^2$  range of the experiments. The data are compared to the QED prediction, equ. 10, neglecting the target photon mass.

DISCUSSION

Question M. Gorn (Munich):

If you had to measure the muon mass from the leptonic structure function  $F_2$ , what would be the uncertainty?

Answer M. Pohl:

I don't know the answer since nobody has tried that up to now. You can see, however, from the error bars in Fig.14 and the logarithmic dependence of  $F_2$  on  $m_\mu$  that the accuracy would not be great.

Question S. Brodsky (SLAC):

One of the best ways to verify that the  $\tau$  is a normal lepton is  $\gamma\gamma \rightarrow \tau^+\tau^-$ . Have such events been identified?

Answer M. Pohl:

No. There is also little hope to do that in the lepton pair final states because of the suppression by the leptonic branching ratio of the  $\tau$  and the indistinct event signatures.

Comment J.H. Field:

The speaker is correct in stating that there is no possibility in extracting the  $\tau\tau$  signal from the  $ee$  and  $\mu\mu$  pair final states. This can, however, be done by using the hadronic decay modes of the  $\tau$  leading to a  $3 + 1$  final state topology.

Comment J. Haissinski (Orsay): The radiative corrections are much larger in the tagged event case than in the no tag case. In the former case, real photon emission by the incoming electron (the one that is scattered at wide angle and tagged) has to be taken into account, not so much because  $\sigma_{tot}$  is changed, but because it modifies the various kinematical distributions. Such corrections have been applied by the CELLO collaboration.

Question P. Kessler : In the CELLO experiment on  $e^+e^- \rightarrow e^+e^- \ell^+\ell^-$ , a rather high asymmetry has been found between  $\ell^+$  and  $\ell^-$ . Can you comment on that? Have the other groups found similar asymmetries?

Answer M. Pohl: QED indeed predicts a small (a few %) forward-backward charge asymmetry coming from an interference between the graphs in Fig. 3a and 3b. CELLO seems to find an asymmetry in their tag data that is higher, but compatible with this prediction. They are, however, not ready to quote a number. In the MARK-J no tag data, i.e. at low  $Q^2$ , the observed asymmetry is very small and compatible with zero.